

Chaos and its characterization in multi-quantum-well laser with periodic-optical pulse injection

GUANG-YU JIANG^{*}, YAN-JUN FU, YAN HUANG, QUAN-SHUI ZHU, MING-GANG CHAI

College of Measuring and Optical Engineering, Nanchang Hangkong University,
Nanchang 330063, China

^{*}Corresponding author: jgy579@126.com

We reveal theoretically chaos and its characterization in a multi-quantum-well (MQW) laser based on periodic-optical pulse injection. Under the effect of periodic-optical pulse injection, the multi-quantum-well laser reveals rich nonlinear dynamics. The results show that the laser can be controlled into single-periodic, dual-periodic, triple-periodic, four-periodic, multi-periodic and chaos for different modulation frequencies and coupling constants; the system has a larger space of parameters.

Keywords: multi-quantum-well (MQW) laser, periodic pulse injection.

1. Introduction

Chaos and its characterization in semiconductor lasers (SLs) have been extensively investigated for its potential applications, such as secured communications, sensors, all-optical frequency conversion, laser chaos-based lidar and radar [1–7]. In the past years, the researchers adopted all kinds of methods for enlarging the modulation bandwidth of laser, where the strongly optical injection locking from another laser was proved to be one of valid approaches [8]. More recently, to enhance the signal transmission rate of SLs in chaos communication system, the bandwidth-enhanced unidirectional chaos synchronization between SLs has been proposed through using the strongly injection-locking technique [9–11], where both the transmitter laser and the receiver laser are respectively subjected to external optical injection from different lasers. Very recently, nonlinear dynamics of semiconductor lasers under repetitive optical pulse injection have also been investigated numerically. Based on these, we modify the systematical frame of [12–15] to the case of multi-quantum-well (MQW) laser in chaos communication system. The optical-pulse-injection induced chaos and its control between a master MQW laser and a slave MQW laser have been investigated

numerically in certain conditions. When the modulation frequencies and the coupling coefficients are changed, the slave laser (SL) shows the rich dynamics, such as single-periodic, dual-periodic, triple-periodic, four-periodic, multi-periodic and chaos.

2. Model

The systematical configuration is depicted in Fig. 1. The chaotic laser system consists of a master MQW laser, optical isolator, optical controller and a slave MQW laser. The light output (E_m) of ML meets the optical isolator, optical controller and modulates SL.

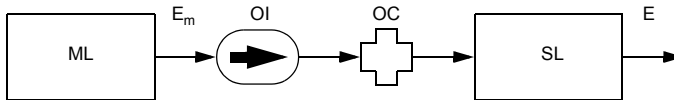


Fig. 1. System configuration in an optically injected MQW laser; OI – optical isolators, OC – optical controller.

Our present study is based on a set of following modified rate equations, including the laser fields E , the phases φ , and the carrier number N in active region. This system can be described by [12, 16, 17]

$$\frac{dE}{dt} = \frac{1}{2}(G - \gamma_p)E + \frac{kE_m F}{\tau_L} \cos(-\varphi) \quad (1)$$

$$\frac{d\varphi}{dt} = \frac{1}{2}\beta_c(G - \gamma_p) + \frac{kE_m F}{\tau_L E} \sin(-\varphi) - \Delta\omega_m \quad (2)$$

$$\frac{dN_B}{dt} = \eta_i \frac{I}{q} - \gamma_{BQ} N_B + \gamma_{QB} N \quad (3)$$

$$\frac{dN}{dt} = \gamma_{BQ} N_B - (\gamma_e + \gamma_{QB})N - G V_p E^2 \quad (4)$$

where E and φ are the slowly varying electric field and phase of the laser optical field, respectively. The parameter $F = \sin(2ft)$ in Eqs. (1) and (2) represents the effect of optical-pulse-injection on SL. The parameter f , is the term governing modulation frequency. N is the carrier number in the laser cavity. The mode gain:

$$G = \frac{\Gamma v_g g_0}{1 + \frac{E^2}{E_S^2}} \log\left(\frac{N + N_s}{N_{th} + N_s}\right)$$

where v_g is the laser cavity photon group velocity, V_p is the volume of laser mode, E_s is the saturation photon field-strength. $N_{\text{th}} = n_{\text{th}}V$ is the carrier number at transparency, n_{th} is the carrier density at transparency. $\gamma_p = v_g(\alpha_m + \alpha_{\text{int}})$ is the total photon loss for the group velocity v_g , the cavity loss α_m and the internal loss α_{int} . $\Delta\omega_m$ is the detuning of the angular frequency between the master and slave lasers. $\tau_l = 2n_g L/c$ is the optical round-trip time in the laser cavity length of L , c is the vacuum speed of light, $n_g = c/v_g$ is the group velocity refractive index. I is the drive current, q is the electronic charge. β_c is the linewidth enhancement factor. η_i is the internal quantum efficiency. γ_{BQ} is the loss of carriers from the barrier region to the well layer and γ_{QB} is the loss of carriers escaping from the well region to the barrier layer. $\gamma_e = A_{\text{nr}} + B(N/V) + C(N/V)^2$ is the nonlinear decay rate of carrier, A_{nr} is the nonradiative recombination rate, B is the radiative recombination factor, C is the Auger recombination factor. k is the optical injection coefficient. The other parameters values used in the calculation are chosen as [12, 16–18]: $L = 1200 \mu\text{m}$, $w = 2\mu\text{m}$, $d = 0.15 \mu\text{m}$, $\Gamma = 0.045$, $n_g = 3.6$, $\alpha_m = 11.5 \text{ cm}^{-1}$, $\alpha_{\text{int}} = 20 \text{ cm}^{-1}$, $\beta_c = 3$, $E_m = 0.126E_s$, $\Delta\omega_m = 4\pi \times 10^9 \text{ rad/s}$, $n_{\text{th}} = 1.2 \times 10^{18} \text{ m}^{-3}$, $A_{\text{nr}} = 1 \times 10^{18} \text{ s}^{-1}$, $B = 1.2 \times 10^{-10} \text{ cm}^3\text{s}^{-1}$, $C = 3.5 \times 10^{-29} \text{ cm}^6\text{s}^{-1}$, $I = 25 \text{ mA}$, $E_s = 1.6619 \times 10^{11} \text{ m}^{-3/2}$, $\alpha = 2.3 \times 10^{-16} \text{ cm}^2$.

3. Results and discussion

The rate equations (1)–(4) can be numerically solved by the fourth-order Runge–Kutta method. To demonstrate and achieve the characterization of optical-pulse-injection induced chaos and its control in multi-quantum-well lasers, the parameters of SL are very important. Therefore, it is necessary to investigate the effects of the parameters on chaos and its control in this scheme; we concentrate on the dynamics for the different k and f , the term governing modulation frequency. Figures 2a–2d represents the time series and phase diagram with different coupling constants for a given frequency. When the modulation frequency f is 1.582 GHz, the SL is controlled to single-

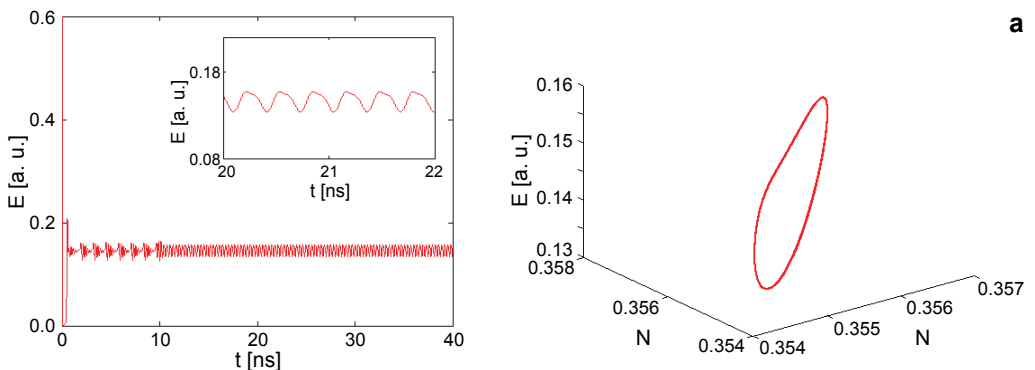


Fig. 2. To be continued on the next page.

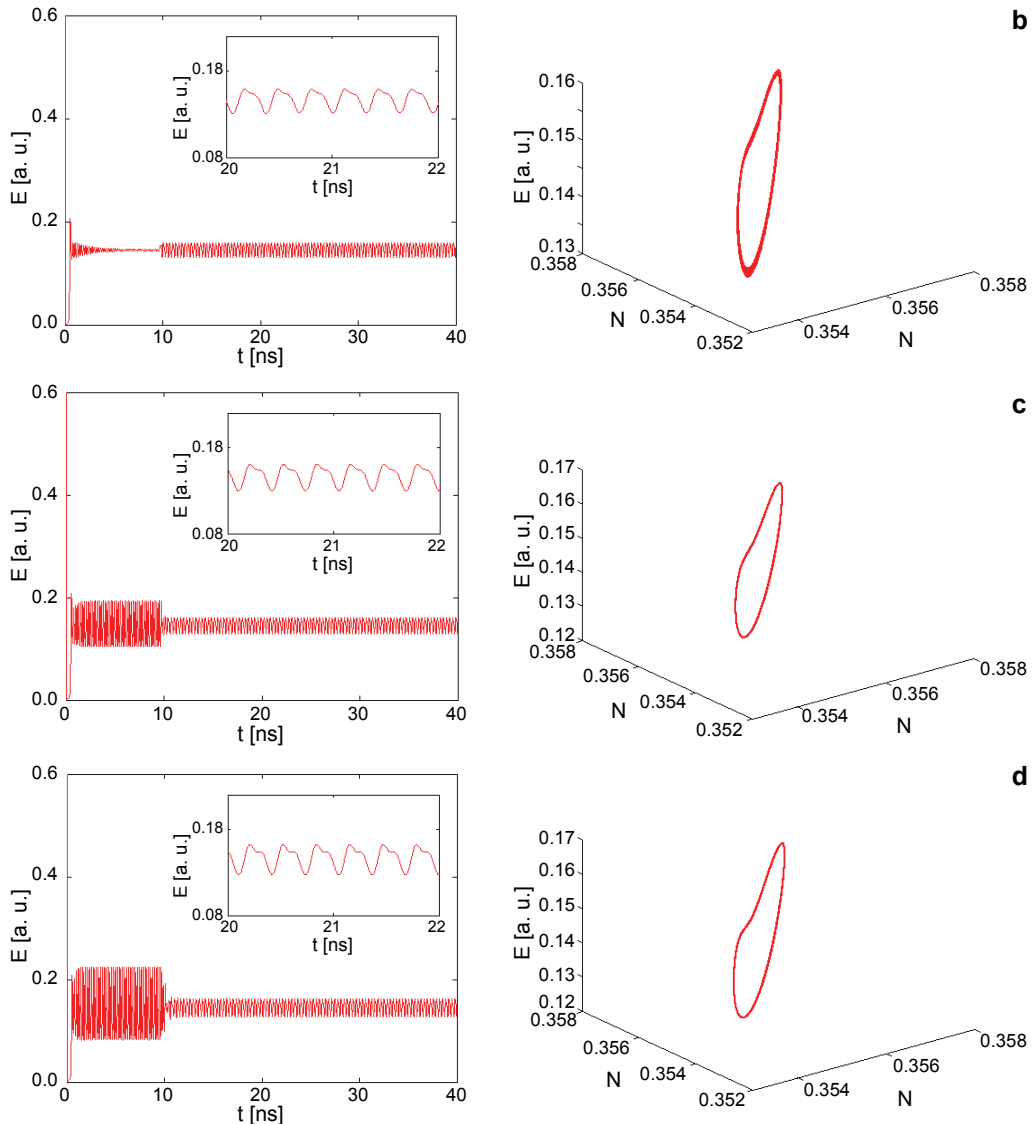


Fig. 2. Time series and phase diagram in SL with different coupling constants for a given modulation frequency.

-cycle for $k = 0.06$. At the increase of k , the time series show a single peak structure, the phase diagram remains unchanged, which shows a steady state (one-cycle) at $k = 0.07$. For $k = 0.08$ and 0.09 , the time series and phase diagram are shown in Fig. 2c and 2d. The laser shows a single-periodic state. The pulse power gradually increases with the increase of the coupling constant.

Under appropriate conditions, the system can produce dual-periodic states by changing different coupling constants for a given modulation frequency $f = 1.216$. Here, we select different injection coefficients; the system can produce several kinds of a two-cycle state, as shown in Fig. 3. From these diagrams, when k is 0.06, the phase portrait and the time series show a two-cycle state. With the increase of $k = 0.0708$, the orbit changes apparently. As $k = 0.08, 0.09$ is further increased, the time series and

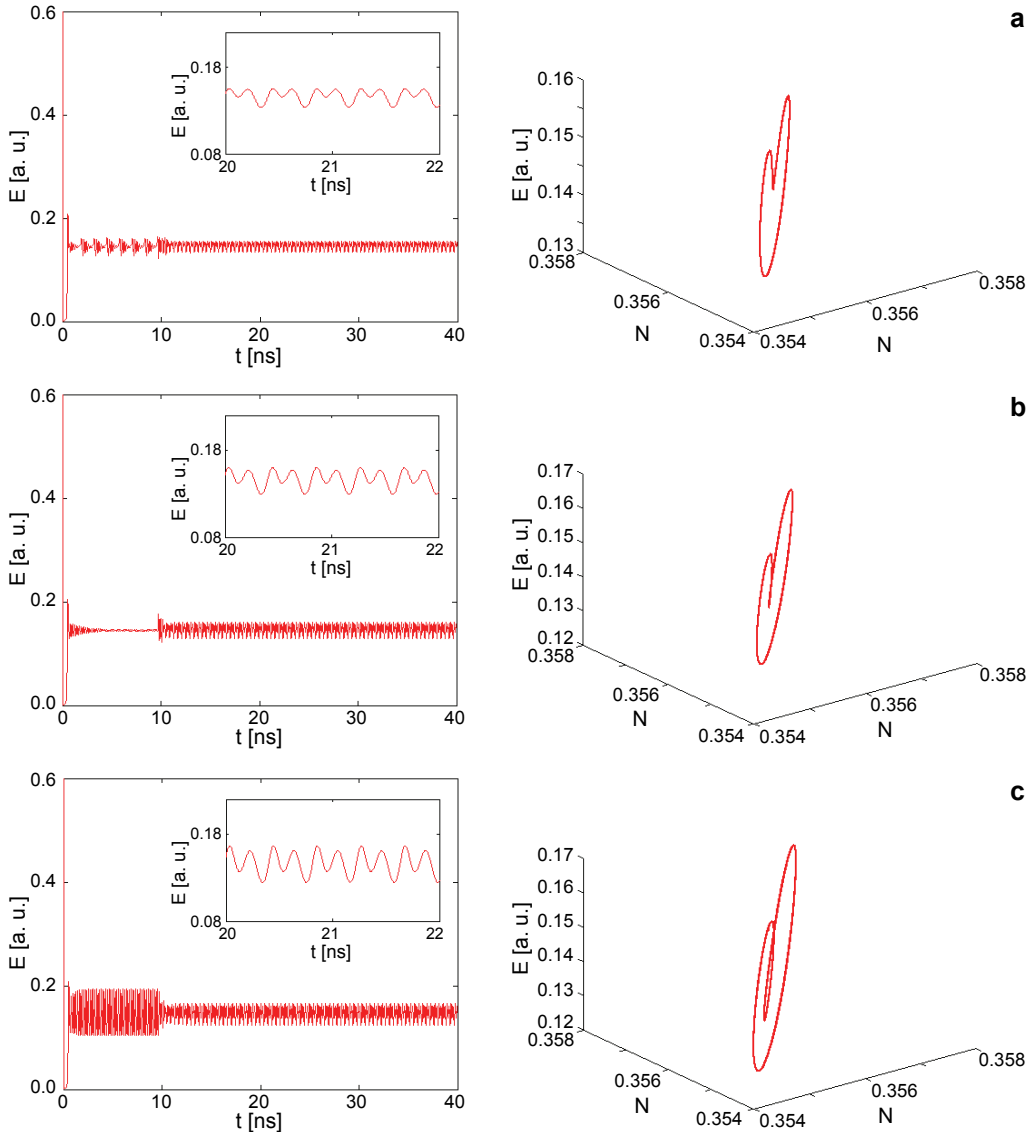


Fig. 3. To be continued on the next page.

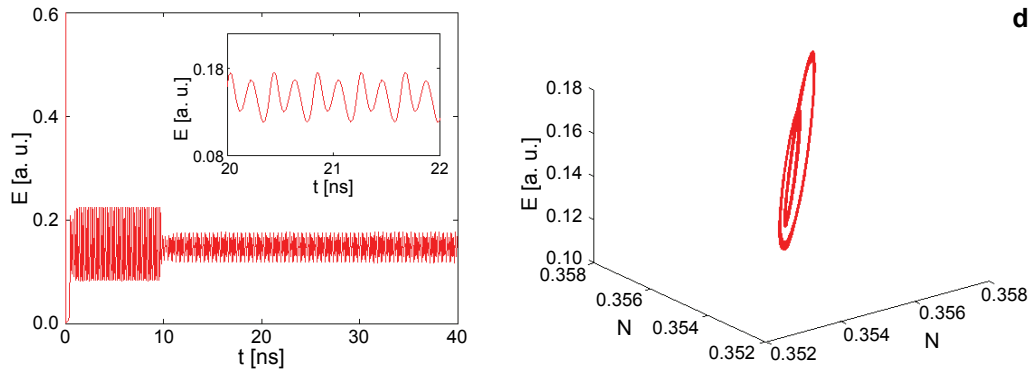


Fig. 3. Time series and phase diagram in SL with different coupling constants for a given modulation frequency.

phase diagram still show a two-cycle state. The results show that every dual-period states can be controlled much easier; the system can be adjusted and controlled in a large parameter range.

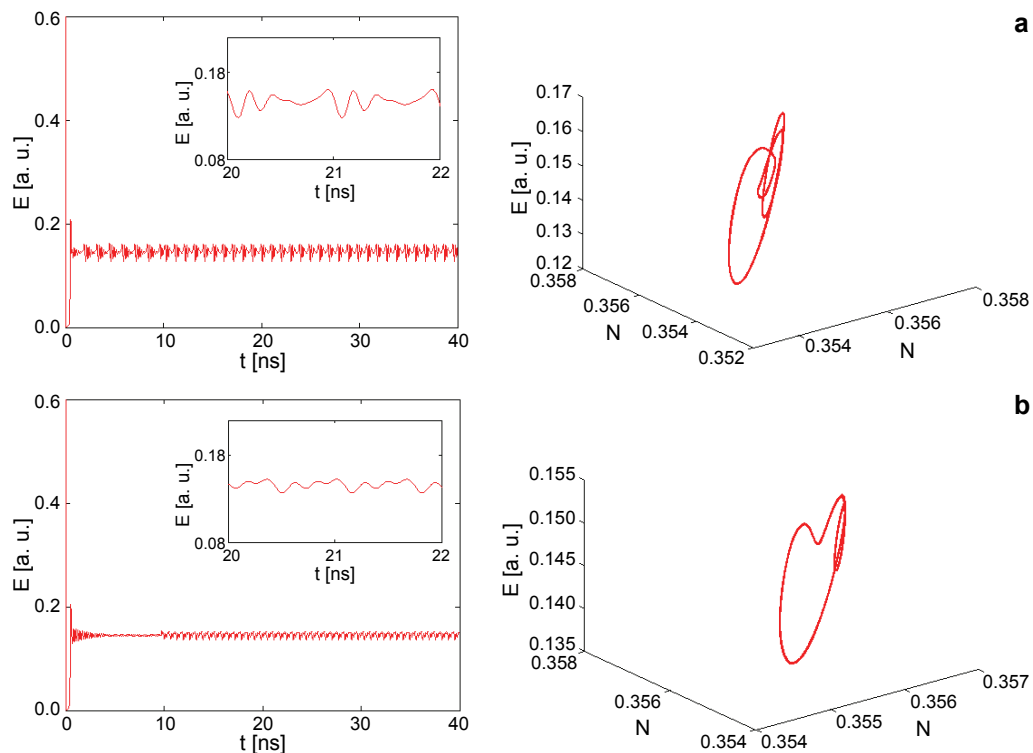


Fig. 4. To be continued on the next page.

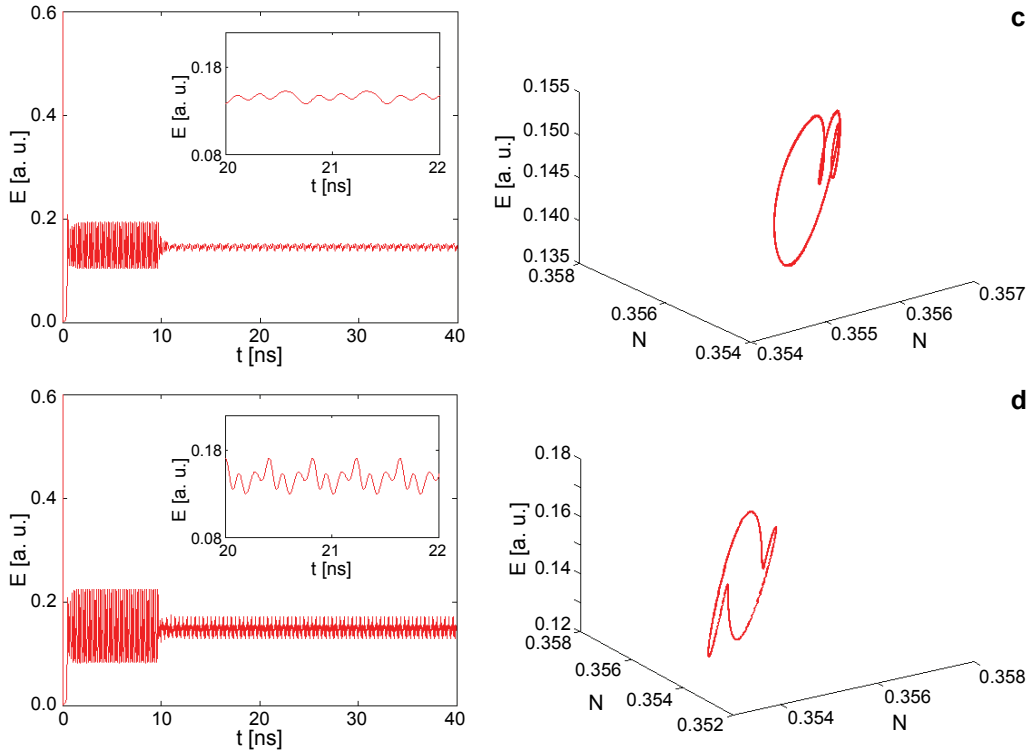


Fig. 4. Triple-periodic states: $k = 0.06$, $f = 0.511$ (a), $k = 0.07$, $f = 0.762$ (b), $k = 0.08$, $f = 0.656$ (c), $k = 0.09$, $f = 4.89$ (d).

Figure 4 shows the time series and phase diagram of the output dynamics versus k at different modulation frequencies. As k is 0.06, the system is a suppressed three-cycle at $f = 0.511$; when k is increased to 0.07, the SL takes on another three-period state, the orbit of the phase diagram changes obviously. As k is increased further, the time series and phase diagram still show a three-period for $k = 0.08$ and $f = 0.656$. Here, we select another group of $k = 0.09$ and $f = 4.89$ GHz; the three-cycle controlled in the system is shown as Fig. 4d. Besides, the pulse power gradually increases with the increase of the coupling constants. Compared with the previous results, Figs. 5a–5c presents time series, phase correlation diagram of the output of SLs for the different coupling constant k at difference modulation frequency f . From these diagrams, the phase portrait shows a four-cycle state, when the coupling constant $k = 0.07$ is taken and the corresponding modulation frequency f is 3.956 GHz. As k is increased, the time series and phase diagram still show a four-period for $k = 0.09$ and $f = 3.96$ GHz. Here, we select another group of $k = 0.1$ and $f = 3.953$ GHz, and the multi-cycle controlled in the system is shown as Fig. 5c. And the pulse power changes apparently. The results indicate that the system based on optical-pulse-

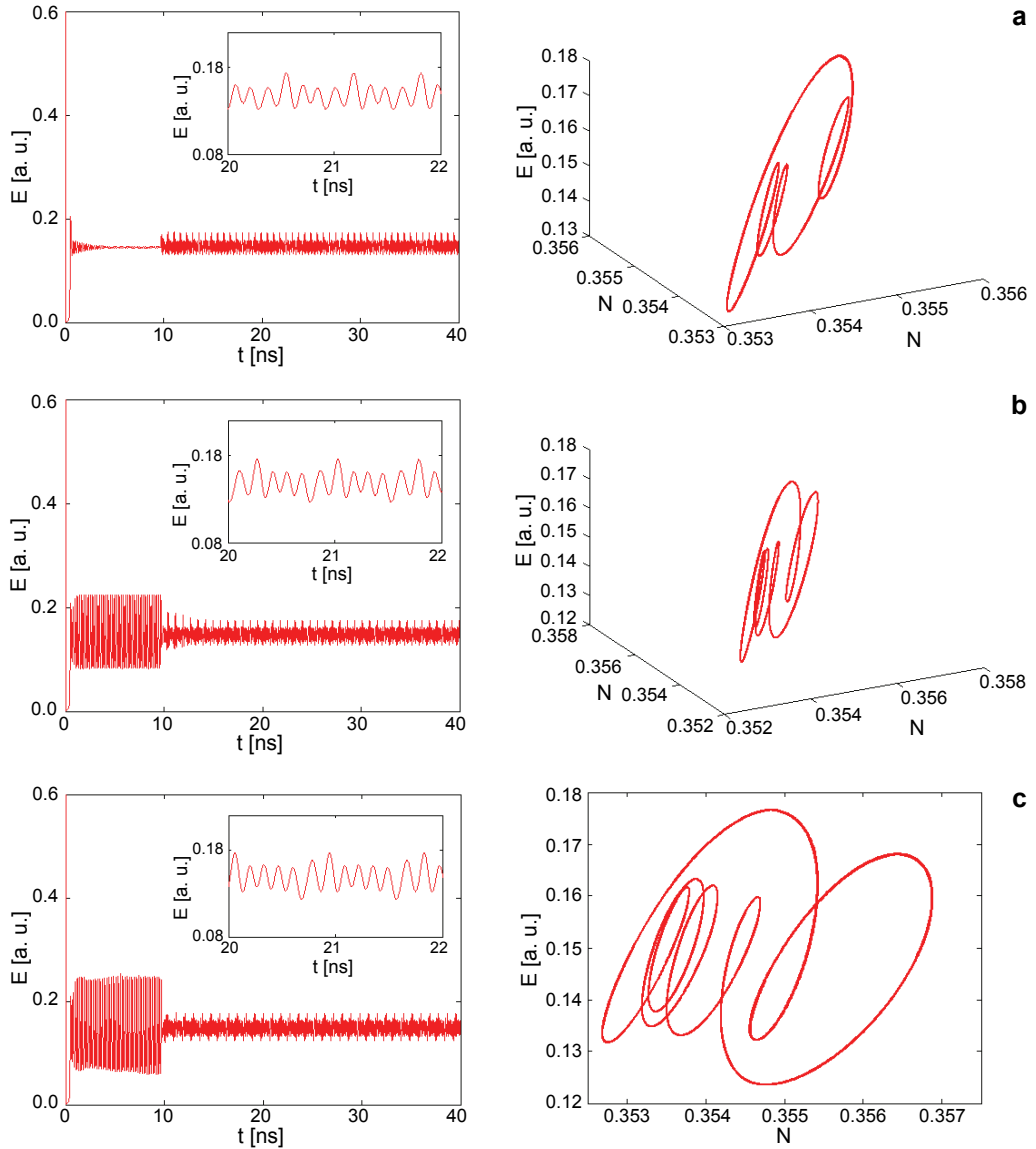


Fig. 5. Multi-periodic states: 4 cycle (a), 5 cycle (b), 6 cycle (c).

-injection easily realizes all types of the three-cycle, four-cycle state and multi-period state by using the different coupling constant k at different modulation frequency f . In addition, the system has a larger space of parameters.

In Figures 5a–5c, as the coupling strengths and modulation frequency are increased further, the time series diagram shows the multi-peak power, and the system is a controlled multi-period state from the phase diagram, namely the system remains the multi-periodic state. Compared with the previous results in Fig. 5, the chaos in

the time series and phase diagram is shown in Figs. 6a–6d. When the modulation frequency f is 5.03 GHz and the coupling constants $k = 0.06, 0.708, 0.08, 0.09$, the system is a controlled chaos from the time series and phase diagram. Figure 7a shows the variation of normalized intensity versus different coupling constants. As the coupling constant increases, the laser is controlled into single-periodic, dual-periodic, triple-periodic, four-periodic, multi-periodic and even chaos for a given modulation frequency. In Figure 7b, when the coupling constant is 0.704, the variation of

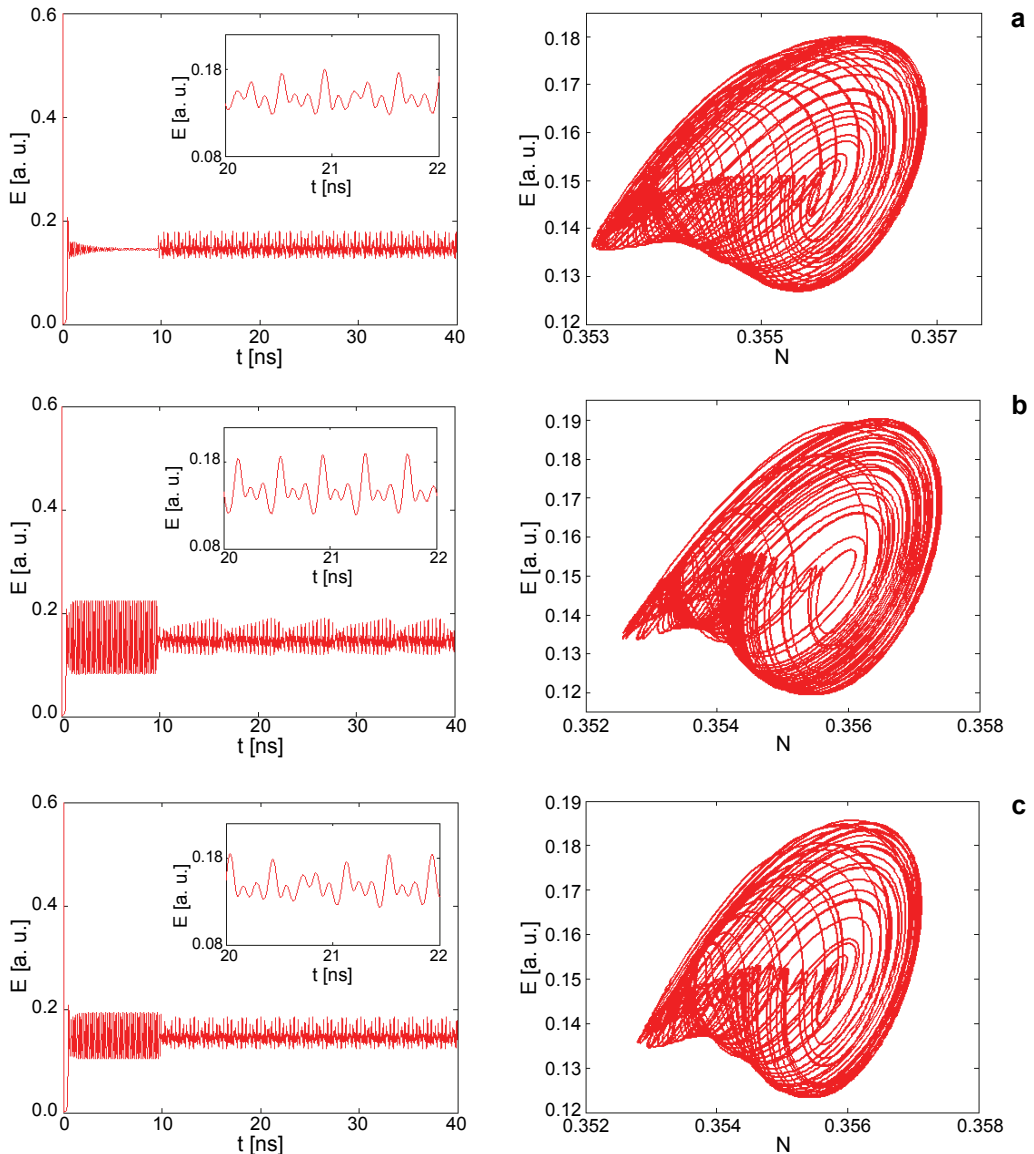


Fig. 6. To be continued on the next page.

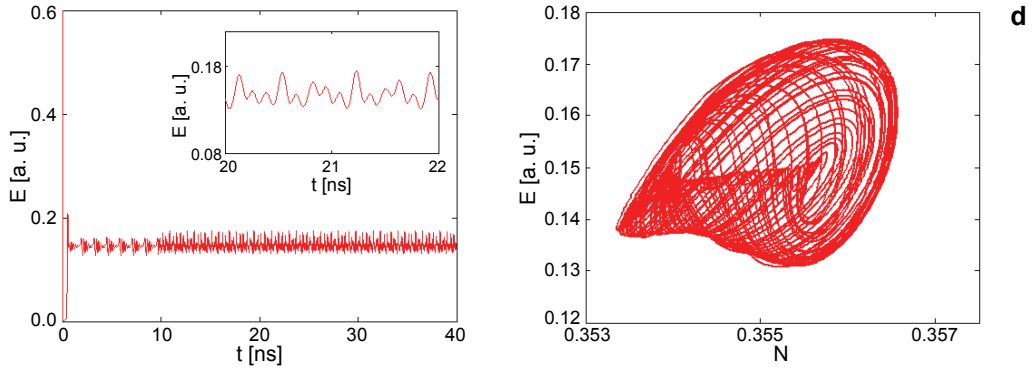


Fig. 6. Chaos states: $k = 0.06$, $f = 5.03$ (a), $k = 0.07$, $f = 5.03$ (b), $k = 0.08$, $f = 5.03$ (c), $k = 0.09$, $f = 5.03$ (d).

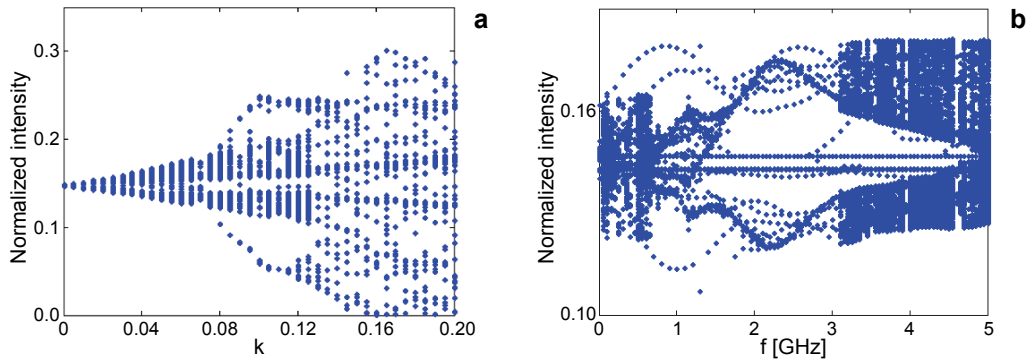


Fig. 7. The variation of normalized intensity versus different coupling constant (a) and modulation frequency (b).

normalized intensity changes with different modulation frequencies. From this figure, we can see that the slave laser shows the rich dynamics, such as single-periodic, dual-periodic, triple-periodic, four-periodic, multi-periodic and chaos for a certain modulation frequency. These results show that there are different ranges of coupling strengths and modulation frequency, which can provide us with different dynamical behaviors. Therefore, by choosing appropriate coupling and modulation frequency values, we can use the method of optical pulse-injection in MQW laser for achieving chaos and suppression of chaos.

4. Conclusions

In conclusion, we present a physical method to realize and achieve chaos and its control between a master multi-quantum-well laser and a slave multi-quantum-well laser

based on optical-pulse-injection. During the process of chaos and its control, the laser exhibits different nonlinear dynamics for different coupling constants and the modulation frequencies of the injected light. The results show that chaos can be controlled and suppressed easily, which can effectively control the system from one-cycle state to multi-cycle states, even chaos. We hope this work would be helpful for an insight into the nonlinear dynamics of the laser in a chaos communication system.

Acknowledgements – This work is funded by the Foundation of Jiangxi Education Bureau (GJJ10192) and Foundation of Key Laboratory of Nondestructive Testing (Ministry of Education) of China (ZD200929001).

References

- [1] HEIL T., MULET J., FISCHER I., MIRASSO C.R., PEIL M., COLET P., ELSASSER W., *ON/OFF phase shift keying for chaos-encrypted communication using external-cavity semiconductor lasers*, IEEE Journal of Quantum Electronics **38**(9), 2002, pp. 1162–1170.
- [2] TANG S., LIU J.M., *Message encoding-decoding at 2.5 Gbits/s through synchronization of chaotic pulsing semiconductor lasers*, Optics Letters **26**(23), 2001, pp. 1843–1845.
- [3] MIN WON LEE, PAUL J., PIERCE I., SHORE K.A., *Frequency-detuned synchronization switching in chaotic DFB laser diodes*, IEEE Journal of Quantum Electronics **41**(3), 2005, pp. 302–307.
- [4] SHENG-KWANG HWANG, HOW-FOO CHEN, CHE-YANG LIN, *All-optical frequency conversion using nonlinear dynamics of semiconductor lasers*, Optics Letters **34**(6), 2009, pp. 812–814.
- [5] FAN-YI LIN, JIA-MING LIU, *Ambiguity functions of laser-based chaotic radar*, IEEE Journal of Quantum Electronics **40**(12), 2004, pp. 1732–1738.
- [6] FAN-YI LIN, SHIOU-YUAN TU, CHIEN-CHIH HUANG, SHU-MING CHANG, *Nonlinear dynamics of semiconductor lasers under repetitive optical pulse injection*, IEEE Journal of Selected Topics in Quantum Electronics **15**(3), 2009, pp. 604–611.
- [7] YU-SHAN JUAN, FAN-YI LIN, *Microwave-frequency-comb generation utilizing a semiconductor laser subject to optical pulse injection from an optoelectronic feedback laser*, Optics Letters **34**(11), 2009, pp. 1636–1638.
- [8] LIN F.Y., LIU J.M., *Harmonic frequency locking in a semiconductor laser with delayed negative optoelectronic feedback*, Applied Physics Letters **81**(17), 2002, pp. 3128–3120.
- [9] XIAOFENG LI, WEI PAN, BIN LUO, DONG MA, *Nonlinear dynamics of two mutually injected external-cavity semiconductor lasers*, Semiconductor Science and Technology **21**(1), 2006, pp. 25–34.
- [10] XIAOFENG LI, WEI PAN, BIN LUO, DONG MA, GUO DENG, *Theoretical analysis of multi-transverse-mode characteristics of vertical-cavity surface-emitting lasers*, Semiconductor Science and Technology **20**(6), 2005, pp. 505–513.
- [11] NING JIANG, WEI PAN, BIN LUO, LIANSHAN YAN, SHUIYING XIANG, LEI YANG, DI ZHENG, NIANQIANG LI, *Influence of injection current on the synchronization and communication performance of closed-loop chaotic semiconductor lasers*, Optics Letters **36**(16), 2011, pp. 3197–3199.
- [12] BENNETT S., SNOWDEN C.M., IEZEKIEL S., *Nonlinear dynamics in directly modulated multiple-quantum-well laser diodes*, IEEE Journal of Quantum Electronics **33**(11), 1997, pp. 2076–2083.
- [13] SENLIN YAN, *Control of chaos in an external-cavity multi-quantum-well laser subjected to dual-wedges and optical dual-feedback*, Chinese Science Bulletin **54**(7), 2009, pp. 1158–1163.
- [14] YAN SEN-LIN, *Bifurcation and locking in an multi-quantum-well laser subjected to external injection*, Optics Communications **282**(17), 2009, pp. 3558–3564.

- [15] YAN SEN LIN, *Control of chaos in an injection multi-quantum well laser via shifting or modulating the injection light*, Journal of Modern Optics **56**(4), 2009, pp. 539–547.
- [16] YAN SEN-LIN, *Study of dual-directional high rate secure communication systems using chaotic multiple-quantum-well lasers*, Chinese Physics **16**(11), 2007, pp. 3271–3278.
- [17] JUANG C., HUANG C.C., HWANG T.M., JUANG J., LIN W.W., *Optoelectronic delayed-feedback and chaos in quantum-well laser diodes*, Optics Communications **192**(1–2), 2001, pp. 77–81.
- [18] LAYEGHI H., ARJMAND M.T., SALARIEH H., ALASTY A., *Stabilizing periodic orbits of chaotic systems using fuzzy adaptive sliding mode control*, Chaos, Solitons and Fractals **37**(4), 2008, pp. 1125–1135.

*Received October 13, 2011
in revised form February 27, 2012*